Journal of University of Science and Technology Beijing
Volume 11, Number 5, October 2004, Page 398

Metallurgy

Formation mechanism of internal cracks in continuously cast slab

Guosen Zhu, Xinhua Wang, Huixiang Yu, Jiongming Zhang, and Wanjun Wang

Metallurgical and Ecological Engineering School, University of Science and Technology Beijing, Beijing 100083, China
(Received 2003-10-17)

Abstract: In order to make clear the formation mechanism of centerline cracks in continuously cast slabs, the form, distribution and other characteristics of the cracks were analyzed. The final solidification point, surface temperature of the slabs and strain in solidifying shell were investigated. The results were that: (1) Five relatively low temperature zones exist on slab surface below the three water spraying nozzles and near the two edges, respectively, which corresponds to the places of centerline cracks and triangle-zone cracks. (2) Centerline cracks and triangle-zone cracks occur because of weak secondary cooling, uneven cooling along slab width, and large variation of roll gap. (3) After minimizing the variation of roll gap and applying the new secondary cooling pattern, the occurring frequency of centerline and triangle-zone cracks minimizes to zero.

Key words: internal crack; continuously cast slab; secondary cooling; solidification; strain

1 Introduction

As a replacement of ingot casting, continuous casting process has been adopted world-widely over last three decades owing to its inherent advantages of low cost, high yield, flexibility of operation, and ability to achieve a high quality of products. However, in recent years, internal cracks have again become an important concern as it was twenty years ago because of higher casting speed, lower manganese content and liquid core reduction technology [1-4].

It has been confirmed by many researchers that bulging and unbending strain are the main causes of intercolumnar cracks, and some factors such as casting speed, intensity of secondary cooling, casting temperature and roll gap have great effects on it [5-10].

K. Miyazawa [6] studied the bulging strain of continuously cast slabs with simple bending theory. He suggested that creep was the dominant deformation mechanism of bulging and the maximum deflection occured near the down roll and increased with the enhancement of roll pitch. A. Grill [7] and B. Barber [8] applied finite element analysis to study the bulging strain. The results were in fair agreement with Miyazawa's.

T.H. Tache [9,10] has systematically studied the unbending strain of continuously cast slabs. The results indicated that unbending strain was not a main reason of intercolumnar cracks when the casting machine was well designed.

J. Miyazaki [11] used bending tests and A. Yamanka [2] used tensile tests to obtain the critical strain for internal crack formation.

Despite such intensive studies, thus far there were few researches on centerline cracks and triangle-zone cracks.

A. Kusano [12] reported that the centerline crack was a shrinkage cavity created through the solidification molten steel closed off in the vicinity of final stage of liquid core. Z.Q. Zeng [13] suggested that intensive cooling at No.1 segment was the main reason of triangle-zone cracks.

In this paper, the formation mechanism of centerline cracks was discussed through analyzing the form, distribution of cracks, measuring the surface temperature and final solidification point, and calculating the total strain and critical strain of solidifying shell. And then prevention methods were put forward.

2 Formation mechanisms of cracks

2.1 Distribution of cracks

Casting conditions was that: the machine type was vertical-curved, the slab thickness was 200-250 mm, the slab width was 1060-1900 mm, casting speed was 0.7-1.4 m/min, the superheat temperature was 15-35°C, the specific cooling water was 0.85-1.10 L/kg. The chemical composition of steel (wt%) is: C, 0.06-

Corresponding author: Guosen Zhu, **E-mail:** zhuguosen2001@yahoo.com.cn

0.20; Si, 0.20-0.30; Mn, 0.35-0.45; P, S<0.020; Als <0.003; T[O]<0.0035; N<0.005.

The distribution of cracks was obtained by analyzing a lot of sulphur print photos of continuously cast slabs (slab size: 1550 mm×230 mm), **figures 1** and **2** show the frequency of cracks occurring at each position. The frequency of cracks was defined as the ratio of defected slabs to total slabs. It can be concluded that along the transverse section of slab, centerline cracks always arise at the center of width and about 450 mm from the center, and triangle-zone cracks arise at about 100 mm from the narrow sides.

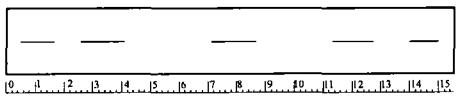

Figure 1 Schematic diagram of locations where cracking occurs.

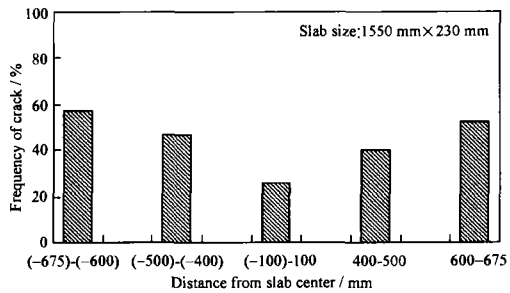

Figure 2 Frequency of crack at different position.

2.2 Final solidification point

As is commonly known, centerline cracks always arise at the final solidification stage. So it is of great importance to find the exact final solidification point. The pin shooting method was applied to measure the thickness of solidifying shell in this paper. After obtaining the shell thickness, the combined solidification coefficient and length of liquid core can be calculated by equations (1) and (2). How to measure the thickness of solidifying shell was introduced by Q.X. Ma [14].

$$K = d\left(\frac{V_c}{L}\right)^{\frac{1}{2}} \tag{1}$$

$$L_c = V_c\left(\frac{D}{2K}\right)^2 \tag{2}$$

where K is the combined solidification coefficient, mm/min$^{1/2}$; d is the measured thickness of solidifying shell, mm; V_c is the casting speed, mm/min; L is the distance of the pin from meniscus, mm; L_c is the distance of the final solidification point from meniscus, mm; D is the thickness of slabs, mm.

The thicknesses of solidifying shell at the position 19.545, 21.614 and 23.679 m from meniscus are 96, 101 and 106 mm respectively. Then K is 24.6 mm/min$^{1/2}$. So the length of liquid core is 27.76 m and the final solidification point lies in segment 14, where there is not water-cooling any more and slabs start to enter air-cooling zone.

2.3 Surface temperature of slabs

The surface temperature of slabs was measured by AGEMA-550 system, which can measure the temperature distribution of one certain area instantaneously.

Figure 3 shows the temperature distribution of a half transverse section of slabs between segment 13 and 14, where LI01 and LI02 represent temperature distribution along line 1 and line 2 in the photo (figure 3(a)), respectively. The results indicate that there are four high temperature zones lying at the places of a quarter of slab width and 150 mm from the narrow side, schematically shown in **figure 4**, where the positions of three spray nozzles are illustrated.

2.4 Strain in the solidifying shell of slabs

The necessary condition of crack formation is that the total strain exceeds the critical strain sustained by solidifying shell. So it is necessary to study the strain under practical conditions. During continuous casting process, three main strains are bulging strain (ε_B), unbending strain (ε_S), and misalignment strain (ε_M).

According to the researches [6,10,15,16], the bulging strain, unbending strain, misalignment strain and the total strain can be calculated by the following equations.

$$\varepsilon_B = \frac{1600S\delta}{l^2} \tag{3}$$

$$\varepsilon_S = 100\times\left(\frac{d}{2}-S\right)\times\left|\frac{1}{R_{n-1}}-\frac{1}{R_n}\right| \tag{4}$$

$$\varepsilon_M = \frac{300S\delta_M}{l^2} \tag{5}$$

$$\varepsilon_T = \varepsilon_B + \varepsilon_S + \varepsilon_M \tag{6}$$

where δ is the bulging amount, mm; S is the shell thickness, mm; l is the roll pitch, mm; d is the slab thickness, mm; R_{n-1}, R_n is the radius of unbending, mm; δ_M is the misalignment among three neighboring rolls, mm; ε_B is the bulging strain; ε_S is the unbending strain; ε_M is the misalignment strain; ε_T is the total strain.

Roll gaps of this continuous casting machine were in-line measured, shown in **figure 5**. The results suggest that under practical conditions, from segment 12

on, the variations of roll gap is positive, varying from 0.5 mm to 3.6 mm. Here variation of roll gap to calculate misalignment strain is supposed as 2.0 mm.

Critical strain calculated according to the results of H. Hiebler [4] is 0.5%.

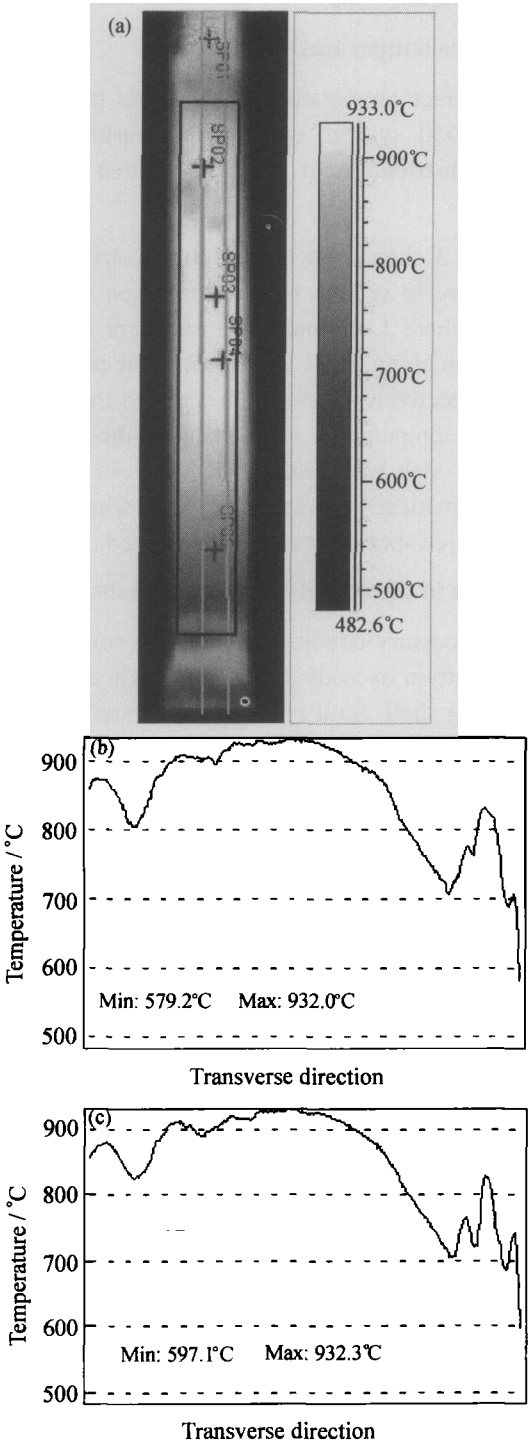

Figure 3 Surface temperature along transverse direction: (a) photo; (b) LI01; (c) LI02.

All strains in the solidifying shell of a slab are shown in **figure 6**. The results indicate that under practical conditions, the total strain exceeds the critical strain and cracks are inevitable results. It also suggests that when the variation of roll gap is big enough, the misalignment strain will be bigger than the bulging strain.

2.5 Causes of cracks

Comparing figure 1 with figure 4, it can be concluded that there must be four high temperature regions and five neighboring lower temperature regions at the final solidification stage. When roll misalignment is big enough, the remaining liquid steel will cause solidifying shell to deform and cracks arise at neighboring lower temperature regions. Then the remaining liquid steel will flow in to fill cracks. But when the temperature is lower than a certain limit which does not allow liquid steel flow freely, liquid steel cannot flow and cracks will remain in slab.

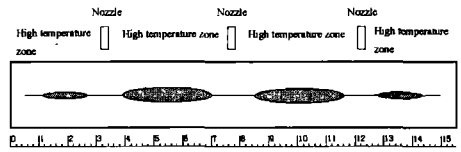

Figure 4 High temperature zones along the traverse section of a slab.

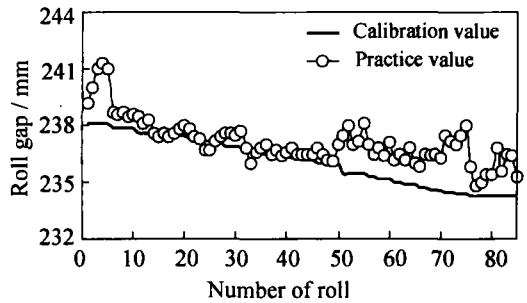

Figure 5 Roll gap of the continuous casting machine.

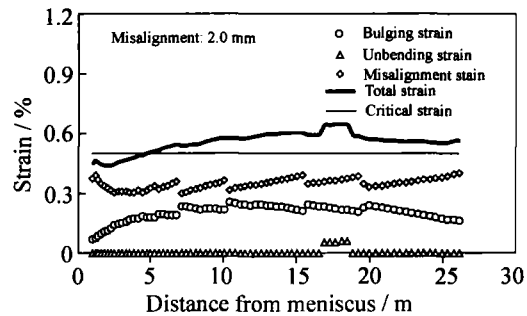

Figure 6 Distribution of strain in solidifying shell.

2.6 Verification of formation mechanism

In order to verify the formation mechanism, four samples with cracks, schematically shown in **figure 7** were torn and analyzed by scanning electron microscope (SEM). **Figure 8** gives SEM photos of fractural surfaces, which suggest that on the fractural surface of place A closest to the high temperature region, there exist a large number of fine and smooth granules ow-

ing to the free shrinkage of solidification which indicates that sample A is well filled by liquid steel. On the fractural surface of sample B, the number of granules is less than that on sample a and the surface of sample B is rugged, which indicates that place B is filled by some liquid steel.

On the fractural surface of samples C and D, there are a lot of shallow dimples. The number of dimples on the former surface is less than that on the later. It indicates that when the crack occurs place C has just finished solidification and place D has already finished solidification completely.

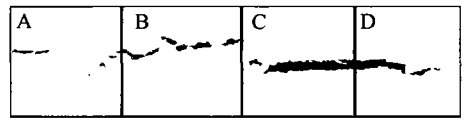

Figure 7 Schematic diagram of sampling.

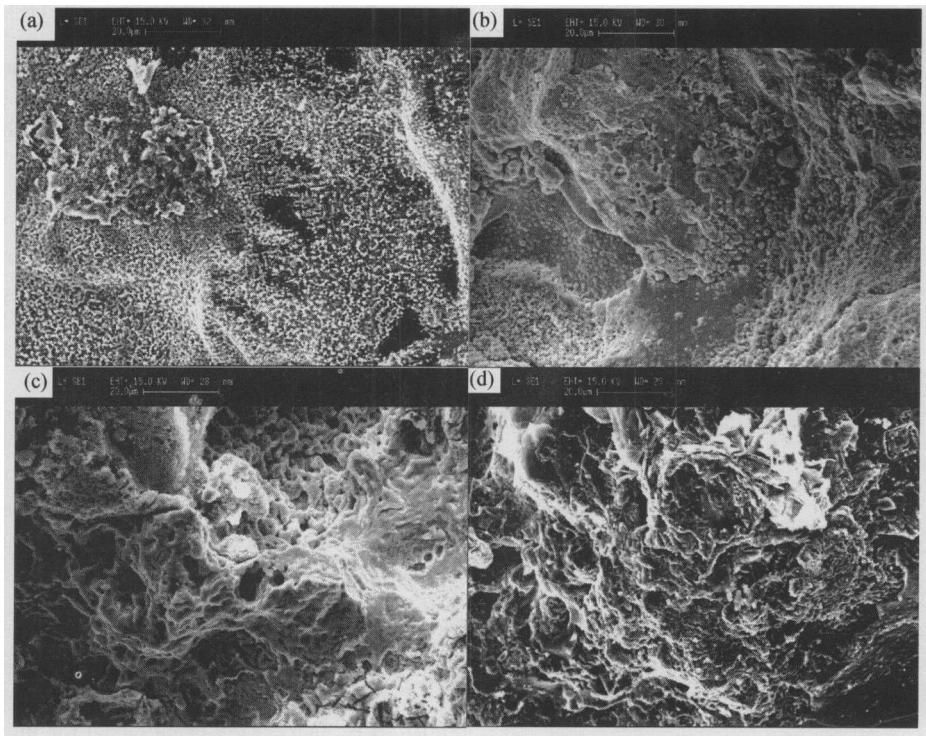

Figure 8 Fractural surfaces of cracks by SEM: (a) sample A; (b) sample B; (c) sample C; (d) sample D.

3 Control of cracks

From the above phenomena, the reasons of crack can be concluded as follows, (1) secondary cooling is too weak, (2) there is serious unevenness of temperature along the transverse section of slabs, and (3) the positive variation of roll gap at the final solidification stage is too large. The first measure to control cracks is to minimize the variation of roll gap to less than 0.5 mm.

The second measure is to design a new secondary cooling pattern. The characteristic of new secondary is to intensify the cooling at the final solidification stage.

Two-dimension unsteady heat transfer phenomena can be represented in terms of the following partial differential equation:

$$\frac{\partial}{\partial x}\left(\lambda\frac{\partial T}{\partial x}\right)+\frac{\partial}{\partial y}\left(\lambda\frac{\partial T}{\partial y}\right)+Q=\rho c\frac{\partial T}{\partial t} \tag{7}$$

where λ is the effective thermal conductivity, $W\cdot m^{-1}\cdot{}^{\circ}C^{-1}$; T is the temperature variable, °C; Q is the latent heat of solidification, $J\cdot kg^{-1}$; ρ is the density of steel, $kg\cdot m^{-3}$; c is the specific heat, $J\cdot kg^{-1}\cdot{}^{\circ}C^{-1}$; t is the time variable, s.

Initial condition $t=0$, $T=1537$°C.

Boundary conditions as the following:

(1) Heat flux density in the mold [3].

$$q=2680-335t^{0.5} \tag{8}$$

(2) Heat transfer coefficient in the second cooling zone [3].

$$h=0.581\times(1-0.0075T_{sur})\times w^{0.451} \tag{9}$$

where w is the flow of cooling water, $L\cdot s^{-1}$; T_{sur} is the surface temperature of a slab, °C.

(3) Heat transfer coefficient in the radiation zone [3].

$$h=\sigma_B\varepsilon_B\left[\left(\frac{T_{sur}+273}{100}\right)^2+\left(\frac{T_a+273}{100}\right)^2\right]\times(T_{sur}+T_a) \tag{10}$$

where σ_B is Stefan-Boltzman constant as 5.67×10^{-8}, $W\cdot m^{-2}\cdot k^{-1}$; ε_B is the blackness of a slab as 0.8; T_a is the temperature of ambient, °C.

Figure 9 gives the calculated and measured temperature of slab surface under the new secondary cooling pattern. The differences between calculated and measured temperatures at four places 13.919, 17.945, 19.555 and 25.744 m from meniscus are 20, 11, 28 and 22°C, respectively. The relative differences are 2.1%, 1.2%, 2.9% and 2.4%.

Figure 10 shows the comparison of surface temperature at the center, a quarter of slab width and 150 mm from the narrow side under the old and new secondary cooling patterns. It suggests that the differences among the center, a quarter of slab width and 150 mm from the narrow side minimize from 57 to 20°C. The new secondary cooling pattern provides even cooling along the transverse section of the slab.

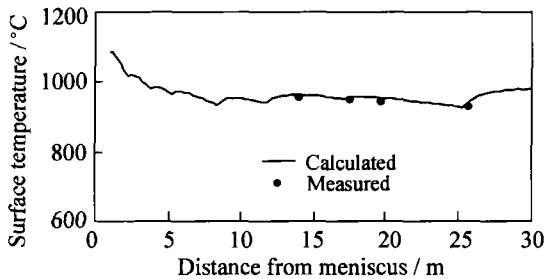

Figure 9 Surface temperature of the slab.

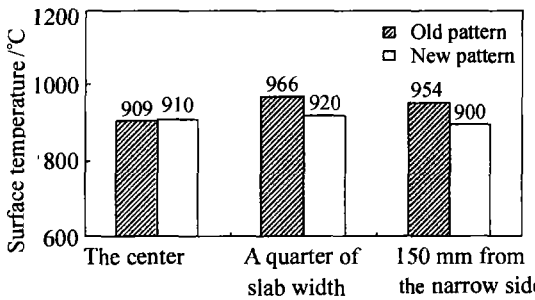

Figure 10 Comparison of surface temperature of the slab.

After minimizing the variation of roll gap and applying the new secondary cooling pattern, the frequency of centerline and triangle-zone cracks minimizes to zero. Furthermore, center segregation is greatly improved.

4 Conclusions

(1) Because of uneven cooling, there are five low temperature zones under three nozzles and two corners, which correspond to the places of cracks.

(2) The causes of cracking can be summed up that uneven secondary cooling along the transverse section of a slab causes uneven solidification, which results in the occurrence of cracks when the variation of roll gap is very large. When the temperature is lower than a certain limit which does not allow liquid steel flow freely, cracks will remain in the slab.

(3) After minimizing the variation of roll gap and applying the new secondary cooling pattern, centerline cracks and triangle-zone cracks disappear.

References

[1] W. Young Mok, H. Heung Nam, and Y. Tae-jung, Analysis of solidification cracking using the specific crack susceptibility [J], *ISIJ Int.*, 40(2000), No.2, p.139.

[2] A. Yamanaka, K. Nakajima, and K. Okamura, Critical strain for internal crack formation in continuous casting [J], *Ironmaking Steelmaking*, 22(1995), No.6, p.508.

[3] G.S. Zhu, X.H. Wang, and H.X. Yu, Strain in solidifying shell of continuous casting slabs [J], *J. Univ. Sci. Technol. Beijing*, 10(2003), No.6, p.26

[4] W. Young Mok, Y. Tae-Jung, and S. Dong Jinl, A new criterion for internal crack formation in continuously cast steels [J], *Metall. Mater. Trans. B*, 31B (2000), p.779.

[5] H. Fujii, T. Ohashi, and T. Hiromoto, On the formation of internal cracks in continuously cast slabs [J], *Tetsu-to-Hagane*, 62(1976), No.14, p.1813.

[6] K. Miyazawa and K. Schwerdtfeger, Computation of bulging of continuously cast slabs with simple bending theory [J], *Ironmaking Steelmaking*, 1979, No.2, p.68.

[7] A. Grill and K. Schwerdtfeger, Finite-element analysis of bulging produced by creep in continuously cast steel slabs [J], *Ironmaking Steelmaking*, 1979, No.3, p.131.

[8] B. Barber, B.A. Lewis, and B.M. Leckenby, Finite-element analysis of strand deformation and strain distribution in solidifying shell during continuous slab casting [J], *Ironmaking Steelmaking*, 12(1985), No.4, p.171.

[9] K.H. Tacke, Muti-beam model for strand straightening in continuous casting [J], *Ironmaking Steelmaking*, 12(1985), No.2, p.87.

[10] M. Deisinger and K.H. Tacke, Unbending of continuously cast slabs with liquid core [J], *Ironmaking Steelmaking*, 24(1997), No.4, p.321

[11] J. Miyazaki, K. Narita, and T. Nozaki, On the internal cracks caused by the bending test of small ingot [J], *Trans. ISIJ*, 21(1981), p. B210.

[12] A. Kusano, H. Misumi, and H. Chiba, The formation mechanism of centerline cracking on the continuous cast slab [J], *Tetsu-to-Hagane*, 84(1998), No.1, p.43.

[13] Z.Q. Zeng, Protection against cracks inside continuous casting slab [J], *Steelmaking* (in Chinese), 33(1998), No.3, p.13.

[14] Q.X. Ma, X.S. Sheng, and X.H. Wang, Experiment on increasing temperature of cc slab for hot charging rolling process [J], *Iron Steel* (in Chinese), 36(2001), No.6, p.20.

[15] H. Fujii, T. Ohashi, and T. Hiromoto, On the formation of internal cracks in continuously cast slabs [J], *Trans. ISIJ*, 18(1978), p.510.

[16] B. Barber, A. Perkins, Strand deformation in continuous casting [J], *Ironmaking Steelmaking*, 16(1989), No.6, p.406.